First principle study of structural, thermal and electronic properties of the chalcopyrites $AlAgX_2$(X=S,Se,Te)

Abstract. First principles density functional theory calculations of structural, thermal and electronic properties of the bulk chalcopyrites $AlAgX_2$ (X=S,Se,Te) were performed using the local density approximation and the modified Becke Johnson approximation. The optimized structure and lattice constants are obtained after a full relaxation of the structure while equilibrium volumes, bulk moduli and derivatives are extracted by fitting the Birch Murnanghan equation of state. For each compound, a systematic study of the density of states, the bandgaps and the band structure was carried out for the different approximations. We found that the modified Becke Johnson approximation gives the most accurate fundamental gap when compared to the experimental data. Phonon frequencies are used to predict the dynamical stability of the structure at the ground state. Thermal properties including free energy and heat capacity are also discussed.

1. Introduction

Increasing energy demand and the search for sustainable, environmental friendly and cheap sources of energy have been a challenge for the scientific community over the last decades. The ternary chalcopyrite semiconductors $A^{I}B^{III}X^{VI}$ (A=Ag,Cu; B=Al,Ga,In; X= O,S,Se,Te) are promising materials to investigate for meeting this challenge. They are also predicted to have potential uses in many other technology applications including low dimensional transistors and optoelectronic devices and photocatalytic splitting [1–3]. Several studies, both experimental and theoretical, have been carried out on these compounds. Hai *et al.* [4] showed from *ab initio* calculations that the bandgaps of $CuInSe_2$ and $CuGaSe_2$ are well predicted by the hybrid functional B3PW91 than any others hybrids functionals. Tsuyoshi *et al.* [5] studied the effect of Cu vacancies on the stability of $CuXSe_2$(X=In,Ga,Al). Lekse *et al.* [6] investigated the effect of the solid state microwave synthesis methods on the purity of $AgInSe_2$.

Our interest in the properties of the $AlAgX_2$(X=S,Se,Te) stems from the fact that in these coumpounds, unlike to the other chalcopyrites families, properties such as vibrational and thermal behaviour have yet not been studied. Moreover, because of the well known problem of discontinuity of the functional derivative on the traditional functionals such as LDA and GGAs, previous studies led to a significant underestimation of the fundamental bandgap [7, 8].

To overcome this issue, more elaborate functionals have been developed including the LDA+U [9], the modified Becke-Johnson functional(MBJ) [10], the hybrid functional HSE [11],

and the GW approach [12]. In first principle calculations, a balance should be found between accuracy of the result and computational time. GW and HSE methods are usually accurate, but are computationally very expensive. Recently, Tran and Balha [10] have developed the MBJ potential which seems to be meeting both requirements and also for a large number of semiconductors and insulators. The MBJ potential is defined as:

$$v_{x,\sigma}^{\mathrm{MBJ}}(\mathbf{r}) = cv_{x,\sigma}^{\mathrm{BR}}(\mathbf{r}) + (3c-2)\frac{1}{\pi}\sqrt{\frac{5}{12}}\sqrt{\frac{2t_\sigma(\mathbf{r})}{\rho_\sigma(\mathbf{r})}}, \tag{1}$$

where $v_{x,\sigma}^{\mathrm{BR}}(\mathbf{r})$ is the Becke-Roussel potential, $\rho_\sigma(\mathbf{r})$ and $t_\sigma(\mathbf{r})$ are the electron and the kinetic energy density. The c parameter depends on the unit cell volume and some free parameters whose values are obtained according to a fit to experimental data.

In this paper, we use the MBJ potential to investigate the bandgaps and the density of states (DOS) of $AlAgX_2$. LDA bandgap is also included for comparison. Dynamical stability and thermal properties are also studied by means of phonon calculations. Our paper is organised as follows: In section 2, we outline the computational method. Section 3 is dedicated to results and discussion while the summary is given in Section 4.

2. Computational details

We employ the first principle DFT method as implemented in the VASP package [13] with inclusion of the plane wave Projector Augmented Wave PAW [14]. To determine the size of the plane wave basis set and **k**-points mesh for sampling the Briouillon Zone (BZ), a series of convergence tests were performed in order to minimize the total energy. We choose a cut-off energy of 520 eV which leds to total energy tolerence of about 0.1 meV. For the integration over the BZ, a Γ-centered Monkhorst-pack grid [15] of $7 \times 7 \times 7$ was found sufficient. The LDA [16] and MBJ are used as exchange-correlation potential. The geometry optimization of the structure and lattice vibrational calculations are performed using LDA only. The linear response method within the density function perturbation theory (DFPT) [17] was used the calculation of phonon and thermal properties The PHONOPY package [18] is used to extract information from DFPT calculations. Initial structures were obtained from Materials Project database [19, 20]. The high symmetry points for plotting the band structure and and phonon dispersion curves were generated using the online version of the AFLOW software [21].

3. Results and discussions

3.1. Structural properties

As with other chalcopyrites, $AlAgX_2$ compounds crystallise in the zincblende structure with the space group $I\bar{4}2d$ (No. 122). In first principle calculation, the geometry optimization and ionic relaxation are performed through a self-consistent minimization of the forces and total energy. Usually, in the construction of the exchange-correlation potentials, the energy is approximated and the potential is then determined as a functional derivative of the energy functional, $V_{xc} = \left(\frac{\delta E_{xc}[n]}{\delta n}\right)$. The MBJ potential was originally constructed as an approximate potential itself [10]. In such cases, it it suggested to use the van Leeuwen-Baerends line integral [22] or the Levy-Perdew virial relation [23] to obtain the energy. Recently, Gaiduk *et al.* showed that the Becke-Jonshon potential doest not satisfy those conditions and therefore is not a functional derivative [24]. Hence for the structural calculations, it is advised to use other functionals. We use the LDA functional for our calculations. Our results are summarized in Table 1 and compared with previous DFT calculations as well as experimental data. The lattice parameters are underestimated because of the well known problem of overbinding in LDA. Nevertheless, our results are within 5% of the experimental values. The slight difference

with other calculated results might come from the method used. Bulk modulus (B_0) and its derivative ($B_0^{'}$) are extracted by fitting the energy per atom and the volume per atom to the Birch Murnangan [25] equation. Results show that these compounds are not hard materials with $AlAgTe_2$ been the softest of the series. We could not find any previous theoretical or experimental values for B_0 and $B_0^{'}$. These results therefore may serve as a reference.

Compounds	Functional	a(Å)	c/a	V_0(Å^3)	B_0(GPa)	B_0'
$AlAgTe_2$	LDA	6.25	1.91	29.04	55.14	4.83
	LDA[a]	6.22	1.97	-	-	-
	Exp[a].	6.29	1.88	29.31	-	-
$AlAgSe_2$	LDA	5.88	1.84	23.36	67.16	4.92
	LDA[a]	5.78	1.99	-	-	-
	Exp[a].	5.95	1.81	23.83	-	-
$AlAgS_2$	LDA	5.61	1.82	20.07	80.5	5.65
	LDA[a]	5.48	1.99	-	-	-
	Exp[a].	5.72	1.77	20.86	-	-

a = Ref. [7]

Table 1: Structural parameters of $AlAgX_2$(X=S,Se,Te) compared to the available experimental and theoretical data.

3.2. Electronic properties

Using the relaxed structures from previous calculations, we calculate the band structure and DOS using MBJ potential. The LDA calculations are also included for comparison. Bandstructures are depicted in Figure 1 and it can be noted that the overall features are similar. The main difference is on the size of the gap. The minimum of the conduction band (MCB) and the maximum of the valence band (MVB) both occur at the Γ point, indicating that these compounds are direct bandgap in the ground state. From Table 2, one can note that LDA dramatically underestimated the bandgap for all the tree compounds. Such behaviour is common to LDA calculations. Previous studies have predicted bangaps in the range of our LDA results (see Table 2). MBJ predicts bandgaps of 3.15 eV, 2.38 eV, and 2.14 eV for $AlAgS_2$, $AlAgSe_2$ and $AlAgTe_2$, respectively. These values are in good agreement with 3.14 eV, 2.55 eV, and 2.27 eV, respectively, obtained from experiment. It is expected that similar results would be obtained with more sophisticated techniques, namely, GW and HSE, but with a very long computational time. The advantage of MBJ is that it combines the accuracy and less computational time. Although the band structure gives information on the size and the nature of the bandgap, it is not obvious to state which orbital contribute to the formation of the bandgap. More details can be obtained from the Density of States (DOS).

Figure 2 displays the partial density of states (PDOS) of the compounds. The conduction band is mainly from Al-p, X-p and Ag-s states. It is worth to note that the small X-p peak which contributes to the formation of the edge of the MCB in $AlAgS_2$ tends to reduce in intensity and shifts to lower energy in $AlAgSe_2$ and does not exist on the $AlAgTe_2$ spectrum. It is rather the Al-p orbital which has the most significant contribution. This could be related to the bond lengths of the chalcogenide atoms with the transition metal atoms which tend to increase with atomic radius and hence, the volume per atom of $AlAgTe_2$ is the largest of the series. We believe such character to be the essence of the narrowing of the bandgap. The edge of the valence band is dominated by Ag-d and X-p orbitals and the strong hybridization between the two orbitals in $AlAgS_2$ reduces gradually in the two other compounds.

3.3. Dynamical stability and thermodynamic properties

Performing phonon calculation is usually a very delicate task because of the difficulty of calculation of the exact force constant acting on an atom. A reliable force constant is usually

Table 2: Bandgap E_g (eV) of $AlAgX_2$ compared to the available experimental and theoretical data. The calculations in Ref. [7] were performed using the tight- bonding linear muffin-tin orbital (TB-LTMO) method.

	$AlAgTe_2$				$AlAgSe_2$				$AlAgS_2$			
	LDA	LDA	MBJ	Exp.	LDA	LDA	MBJ	Exp.	LDA	LDA	MBJ	Exp.
E_g(eV)	1.12	1.36[a]	2.14	2.27[a]	1.07	1.59[a]	2.38	2.55[a]	1.83	1.98[a]	3.15	3.13[a]

a = Ref. [7],

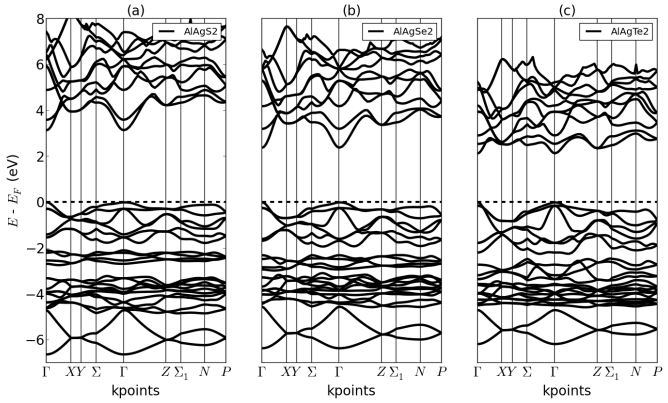

Figure 1: Band structure of $AlAgX_2$ calculated using MBJ. Both the minimum conduction and maxi,um valence band occur at the Γ point indicating a direct bandgap for all the compounds.

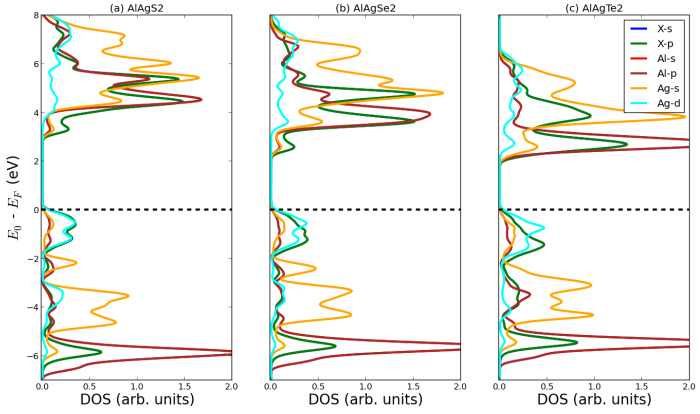

Figure 2: (Colour online) Density of states of $AlAgX_2$. The Fermi level E_F is shifted to zero.

obtained by using a supercell since in the normal unit cell, interaction between the displaced atoms and their images is important. A supercell of 64 atoms and with a $2 \times 2 \times 2$ **k**-points grid were used for our calculations. The calculations should also meet the total energy convergence criterion. Hence because of the non existence of MBJ exchange correlation energy as stated above, LDA is used as exchange correlation functional. A structure is predicted to be stable with respect to phonon when no vibration modes have imaginary real frequencies.. The phonon

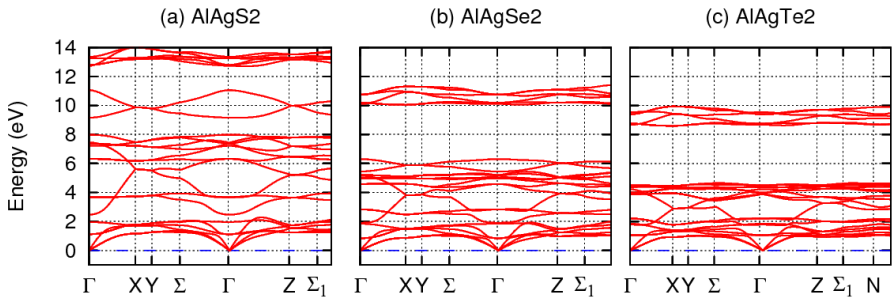

Figure 3: (Colour online) The phonon-dispersion curves of $AlAgX_2$.

spectrum along the high symmetry points is depicted in Figure 3. A careful observation shows that apart from the acoustic modes going to zero frequencies around the Γ point, all the phonon-dispersion curves remain positive throughout the BZ attesting to the stability of the structures. Moreover, there is not a clear limit between the acoustic and the optical modes for all the three spectra with $AlAgS_2$ having the highest optical modes.

Phonons contribute to a range of thermodynamic properties including Helmholtz free energy $F(T)$, entropy $S(T)$ and heat capacity at constant volume $C_v(T)$. $F(T)$ and $C_v(T)$ are displayed in Fig.(4) up to $1000K$. In this temperature range, it is assumed that phonon interactions is still small such that anharmonic interaction are not occurring yet. The Helmholtz free energy is defined as $F = U - TS$ with U the internal energy. Since entropy S is an increasing function of the temperature, F should decrease with increment of temperature. All the three compounds satisfy that condition. $F(T)$ does not go to zero at $0K$ indicating a zero point motion in the systems. $C_v(T)$ increases rapidly at lower energy $[0 - 200K]$ as predicted in the *Debye model* [26]. From the room temperature $\sim 300K$, it converges to a limit close to $200J/K.mol$. This asymptotic behaviour is in agreement with the *Dulong-Petit law* which states that $C_v(T)$ should tend to $3Rn$ at high temperature with $R = 8.31J/K.mol$ the gas constant and n the number of atom in the unit cell [26]. Each of our unit cells has $n = 8$ atoms and leads to $C_v(T) \simeq 199,44J/K.mol$ which corresponds to the limit obtained in Fig.(4-b).

Many factors contribute to the heat capacity and are of varying importance. For insulators and semiconductors, the principal contribution comes from lattices vibration at low temperature. By increasing the temperature, electrons get excited and their contribution cannot be neglected. The population of electrons in the conduction band starts increasing when the thermal energy K_BT (K_B, the Boltzmann constant) approaches the energy gap ($K_BT \sim E_g$). The maximum temperature in our study was set at $500K$ which leads to a thermal energy of 0.042 eV. This value is lower than all the calculated bandgaps. We can conclude that up to $500K$, the phonon contribution to C_v is still the most important for the compounds under investigation.

4. Conclusion

In this work, we have studied the structural, electronic and thermal properties of the chalcopyrites $AlAgX_2$ (X=S,Se,Te) using LDA and MBJ approximations. In spite of the overbonding in LDA, lattice parameters obtained from our calculations were in the range of experimental values. Band structures spectrum show that all the three compounds have a direct bandgap. By the mean of the MBJ potential. we obtained very accurate bandgaps compared to experimental data. The advantage of using the MBJ is that it is known to be as cheap as LDA and GGAs in term of computationally time. Similar agreement with experimental data is usually obtained with very computational expensive methods such as HSE and GW methods. The PDOS spectra show that the p orbitals from chalcogenide and Al atoms contribute significantly to the

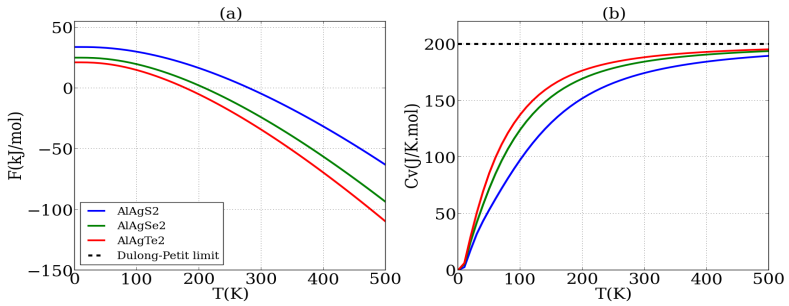

Figure 4: (Colour online) Free energy and Heat capacity of $AlAgX_2$.

formation of the MCB and therefore are at the essence of the bandgap difference between the three compounds. Using the supercell methods with the DFPT, we study the dynamic stability of $AlAgX_2$. Because of the absence of negative frequencies along the phonon-dispersion curves, $AlAgX_2$ are predicted to be dynamically stable at the ground state. Heat capacity follow the Debye model at low temperature and converges to the Dulong-Petit limit at high temperature.

Acknowledgements

This work was partially supported by DAAD-AIMS (African Institute for Mathematical Sciences) scholarship. The Centre for High Performance Computing (CHPC), Cape Town-South Africa is thanked for the computational resources.

References

[1] Reshak A 2013 *Int.J. Electrochem. Sci.* **8** 9371–9383
[2] Zunger A and Jaffe J 1983 *Phys. Rev. Lett.* **51** 662–665
[3] Jaffe J and Zunger A 1984 *Phys. Rev. B* **29** 1882–1906
[4] Xiao H, Tahir-Kheli J and Goddard III W A 2011 *J. Phys. Chem. Lett.* **2** 212–217
[5] Maeda T and Wada T 2005 *J. Phys. Chem. Sol.* **66** 1924–1927
[6] Lekse J W, Pischera A M and Aitken J A 2007 *Mater. Res. Bull.* **42** 395–403
[7] Mishra S and Ganguli B 2011 *Solid State Commum.* **151** 523–528
[8] Jayalakshmi V, Mageswari S and Palanivel B 2012 *Solid State Phys. Proc.* **1447** 1087–1088
[9] Anisimov V I, Zaanen J and Andersen O K 1991 *Phys. Rev. B* **44** 943–954
[10] Tran F and Blaha P 2009 *Phys. Rev. Lett.* **102** 226401
[11] Heyd J, Scuseria G E and Ernzerhof M 2003 *J. Chem. Phys.* **118** 8207–8215
[12] Shishkin M and Kresse G 2007 *Phys. Rev. B* **75** 235102
[13] Kresse G and Furthmüller J 1996 *Phys. Rev. B* **54** 11169–11186
[14] Kresse G and Joubert D 1999 *Phys. Rev. B* **59** 1758–1775
[15] Monkhorst H J and Pack J D 1976 *Phys. Rev. B* **13** 5188–5192
[16] Perdew J P and Wang Y 1992 *Phys. Rev. B* **45** 13244–13249
[17] Baroni S, de Gironcoli S, Dal Corso A and Giannozzi P 2001 *Rev. Mod. Phys.* **73** 515
[18] Togo A, Oba F and Tanaka I 2008 *Phys. Rev. B* **78** 134106
[19] Belsky A, Hellenbrandt M, Karen V L and Luksch P 2002 *Acta Crystallogr., Sect. B: Struct. Sci* **58** 364–369
[20] Jain A, Ong S P, Hautier G, Chen W, Richards W D, Dacek S, Cholia S, Gunter D, Skinner D, Ceder G and Persson K a 2013 *Appl. Phys. Lett. Mater.* **1** 011002
[21] Curtarolo S, Setyawan W, Hart G L, Jahnatek M, Chepulskii R V, Taylor R H, Wang S, Xue J, Yang K, Levy O *et al.* 2012 *Comput. Mater. Sci.* **58** 218–226
[22] van Leeuwen R and Baerends E J 1995 *Phys Rev. A* **51** 170–178
[23] Gross E K and Dreizler R M pp 11–31, 1995 *Density Functional Theory* (Springer)
[24] Gaiduk A P and Staroverov V N 2009 *J. Chem. Phys* **131** 044107
[25] Birch F 1947 *Phys Rev.* **71** 809–824
[26] Kittel C and McEuen P 1986 *Introduction to solid state physics* vol 8 (Wiley New York)